Influence of bionic non-smooth surface texture on tribological characteristics of carbon-fiber-reinforced polyetheretherketone under seawater lubrication

Zhiqiang Wang[a,b,c*], Qi Fu [a], Robert J. K. Wood[c], Jun Wu [c], Shuncai Wang[c]

[a]School of Mechanical Engineering, Hangzhou Dianzi University, Hangzhou, China

[b]School of Mechanical Engineering, Zhejiang University, Hangzhou, China

[c]National Centre for Advanced Tribology at Southampton (nCATS), University of Southampton, Highfield, Southampton, UK

Abstract

To explore anti-wear characteristics for valve pair, the influences of smooth and non-smooth surfaces on tribological properties of the carbon-fiber-reinforced polyetheretherketone (CFRPEEK) coupled with stainless steel 316L were investigated under natural seawater lubrication. The results show that the specimen with ellipsoidal pits has the best frictional performance, followed by the specimen with triangular pits, and the specimen with hemispherical pits is the worst. Microscope observation analysis showed that the reasonable non-smooth surface can reduce adhesion wear and improved the stability of friction system as compared to smooth surface. Results also indicated that the reasonable non-smooth unit can effectively store seawater and debris, and produce hydrodynamic lubrication effect, which surface shows the excellent tribological properties.

Keywords: Bionic non-smooth surface; Friction and wear; Seawater lubrication; Carbon-fiber-reinforced polyetheretherketone

1. Introduction

Due to the special physical and chemical properties of seawater, valve pairs of water hydraulic motor that are usually working in gear under seawater situation are prone to failure due to corrosion, friction and wear. At present, the main approaches to improving the corrosion resistance and wear resistance of valve pairs are to adopt new materials, new processes, new structural design, or improve the hardness of materials and carry out surface coating, but it is very difficult to further improve the tribological characteristics [1-4]. On the contrary, the bionic non-smooth surface effect has great potential to improve the lubrication, reduce the viscosity and

* Corresponding author. Tel/Fax: +86 571 86878677. E-mail address: wzq78452501@163.com (ZQ. Wang).

resistance and enhance wear resistance of friction pairs.

A large number of organisms, such as sharks, beetles and snakes, have been observed and studied and it has been found that these organisms generally have excellent functions of desorption, adhesion reduction, drag reduction and wear resistance [5-7]. These functions are closely related to the non-smooth morphology of the body surface. In order to improve the lubricity and wear resistance of the working surface of the moving pairs, the non-smooth morphology of the biological surface with wear resistance is applied to various surfaces of mechanical parts with relative movement, which takes advantage of the bionic non-smooth surface effect. This effect has been effectively applied in many situations in order to improve the tribological performance, especially to reduce friction in mechanical components, such as bearings [8], piston rings [9], mechanical seals [10], and cutting tools [11].

Generally, there are two main aspects in tribological performance where surface texture plays an active role. Firstly, surface texture can store up the lubricants and thus offer sustainable lubrication; secondly, it can capture debris generated during service and thus minimize abrasive wear [12-14]. There are three major parameters related to surface texture, that is, dimple shape, dimple depth and dimple density [15]. Wakuda et al. [12] tested the sliding of steel pins on textured ceramic plates, finding that the reduction of the friction coefficient showed great dependence on the size and density of the texture features. Sunet al. [16] produced six types of micro-textures with different diameters and area densities on the surfaces of the TC11 alloy and found that a micro-dimpled structure with relatively small diameter and high density was likely to improve the tribological properties of TC11 alloy at 500℃. Woset al. [17] investigated the effect of textured surfaces on the improvement of tribological properties of sliding elements using a pin-on-disc tester under conformal contact starved lubrication. And it was concluded that tribological behaviors of sliding pairs with one sample textured were better than those with both samples textured for large area densities and the increase of area ratio of pits would bring about better stabilization of the friction force.

It is recognized that the geometry of dimples can be a major factor influencing frictional behaviors [18]. However, the mechanisms behind are still unclear. Qiu et al.

[19] evaluated the friction coefficient and stiffness of gas-lubricated textured parallel slider bearings with six different texture shapes. And the ellipsoidal shape was found to yield the minimum friction coefficient and the highest bearing stiffness regardless of the operating conditions. Chenet al. [20] experimentally investigated the effect of triangular surface texture on the friction and wear properties of the die steel substrate with TiN coatings under oil lubrication. The results showed that the combined method of surface texturing process and surface coating process generated more excellent tribological properties (the lower frictional coefficient and wear) than the single texturing process or the single coating process. A series of experiments were conducted by Qiu [21] to examine the frictional characteristics of laser surface texture with two dimple shapes (circular and elliptical). It was found that the specimens with surface texture provided low coefficient of friction (COF) compared with plain (dimple-free) surfaces and the dimples of elliptic shape provided lower COF than that of circular shape in the tested environment. An experimental and numerical study of the lubrication effectiveness of textured surfaces with dimples with different shapes was conducted by Shen [22]. It was showed that the shape of the dimples had a profound influence on the load-carrying capacity. To be specific, cylindrical dimples with rectangular cross-section produced stronger load-carrying capacity than those with triangular cross-section. To optimize the shape of dimple surface texture under unidirectional sliding, a numerical approach developed based on a Genetic Algorithm to improve the tribological performance was proposed by Zhang[14]. It was illustrated that textures of the bullet and fish shapes had lower friction coefficient than those of circular shape. To summarize, although satisfactory results have been obtained, to findthe optimal parameters for the textureis still very challenging due to alarge number of variables involved and the complexity of control. In addition, the optimal design of texture seems to be highly dependent on the type of contact and operating conditions; and in certain cases, some textures have been reported to lead to detrimental consequences, if designed improperly [23-24].

According to the literature, almost all of the studies presented the textures on the scale of micron or nano. However, some scholars have found that micro-pores can not

increase the hydrodynamic effect due to the great pressure of fluid medium, while the macro texture can not only greatly improve this effect but also increase stiffness [25-26]. Nowadays, methods of fabricating surface textures can be generally classified into mechanical method [27], ion beam texturing method [28], etching method [29] and energy beam method [30]. Among these methods, laser surface texturing (LST) is consideredas the most promising texturing technology [31]. The main reason is that the fabrication of textures by LST can be precisely controlled and environmentally friendly [32]. Especially, the macro texturing can rely on digital machining, which can prevent the textured surface from laser thermal shock while creating more complex shapes.

Although there have been many studies on non-smooth surface, they are mainly focused on the experimental study under conditions of dry friction, grease lubrication, solid lubrication or water lubrication. By comparison, the effect of surface texture with different shapes and geometries on tribological characteristics between the friction pairs under seawater lubrication has rarely been reported. In this paper, to explore the tribological characteristics of the end-face valve pair of seawater hydraulic motor, different types of bionic non-smooth macro units were processed on the surface of CFR/PEEK specimens using CNC machine tool and the friction pair was formed after coupling with another surface of 316L stainless steel. To study the friction and wear properties of bionic non-smooth surfaces with different morphologies under seawater lubrication, the relative rotating process of valve pairs in seawater was simulated by MMD-5A end-face wear tester, and the three-dimensional topography and roughness of all specimens before and after the experiment were observed by optical three-dimensional surface measuring instrument. Finally, some results were obtained and discussed.

2. Experimental Materials and Method

2.1 Materials and Specimens

In order to better explore the influence of non-smooth surface on the friction and wear performance of the valve plate, the research was carried out on the basis of selecting the optimum matching material [3,33,34]. The material of the upper specimen was taken from the commonly-used 316L stainless steel because the steel, having excellent pitting corrosion resistance and having the capability of being stably used in halogen ion environment such as chloride ion, is commonly used in marine

environment. The main performance parameters of 316L stainless steel were shown in Table 1.

Table 1 Property parameters of 316L stainless steel

Parameters/ Unit	Value
Density / (g·cm−3)	8.03
Elasticity modulus / GPa	206
Brinell hardness / HB	230
Elongation / %	30
Tensile strength / MPa	620
Yield strength / MPa	310

The material of the lower specimen was taken from CFRPEEK, which can be used in marine environment owing to its low friction coefficient, excellent mechanical and corrosion resistance. The substrate, polyetheretherketone (PEEK), of the lower specimens is white powder with average particle size of 10 μm and density of 1.32 g/cm^3. The reinforcements are short-cut carbon fibers with a diameter of 7 μm, density of 1.75 g/cm^3, tensile strength of 3.5 GPa and tensile modulus of 228 GPa. Firstly, the short-cut carbon fibers were immersed in acetone for 48 hours, then ultrasonically stirred with mixed acid (98% sulphuric acid: 69% nitric acid = 3:2) for 20 minutes. After being cleaned with distilled water, the short carbon fibers were dried off in an oven at 150 ℃ for 6 hours before being taken out. Then the carbon fiber and PEEK were fully mixed with a volume ratioof 3:7 and placed in a mould of the hot press. After being compacted, heated up (375~390℃) and pressed(10~14MPa), pressure release, exhausted, cooled and demoulded, the material for the lower specimen was obtained. The main performance parameters of CFRPEEK were shown in Table 2.

Table 2 Property parameters of CFRPEEK

Parameters/ Unit	Value
Density / (g·cm−3)	1.4
Water absorption (24 h) / %	0.06
Rockwell hardness / HRR	107
Tensile strength / MPa	220
Bending strength / MPa	298
Compressive strength / MPa	240

2.2 Shape and geometric characteristics

For the sake ofliving in a complex environment for a long time, organisms will inevitably be affected by friction, so that the non-smooth surfaces of some organisms gradually possess the function of resistance reduction and wear resistance in the process of evolution. However, the surface morphology of different organisms has significant differences. For example, the snake [5], as a very adaptable reptile, will suffer from wear and tear when moving through grass, trees, deserts, swamps, and the sea. To overcome these, some scales on the body surfaces of snakes have evolved into a triangular shape, as shown in Fig. 1(a), so that the friction resistance is reduced because its non-smooth surface destroys the continuous friction process. The cytister bengalensis [35], a kind of aquatic and terrestrial insect, is also one of the insects that swim the fastest in the water. The reason why the cytister bengalensis can adapt to such a changeable living environment, especially swim fast in water, is closely related to its special body surface morphological structure. This non-smooth body surface has a significant effect of drag reduction when the cytister bengalensisis is flying in the air or swimming in water. It can be seen from Fig. 1.(b) that there are many ellipsoidal pits on the body surface of the cytister bengalensis. In addition to the effect of drag reduction mentioned above, it has been found that golf balls with circular pits, as shown in Fig. 1(c), can fly farther than those with smooth surfaces. The reason is that the circular pits on the surface of golf balls greatly reduce the aerodynamic drag they are subjected to when the balls are flying in the air and at the same time, the lift force of the golf ball is gradually increased as the rotation of the ball [36]. Inspired by the rough surfaces of snakes, cytister bengalensises and golf balls, three bionic non-smooth surfaces with hemispherical pits, triangular pits and ellipsoidal pits, respectively were designed for the lower specimens.

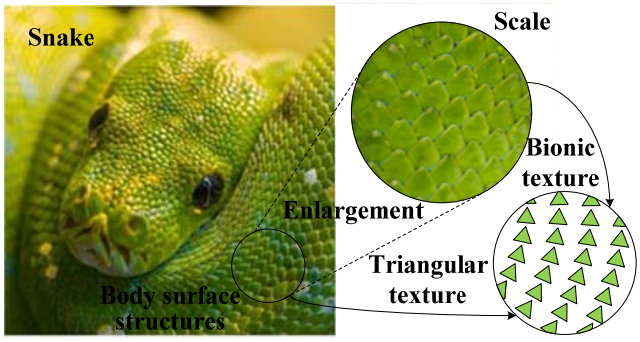

(a) The snake and its body surface

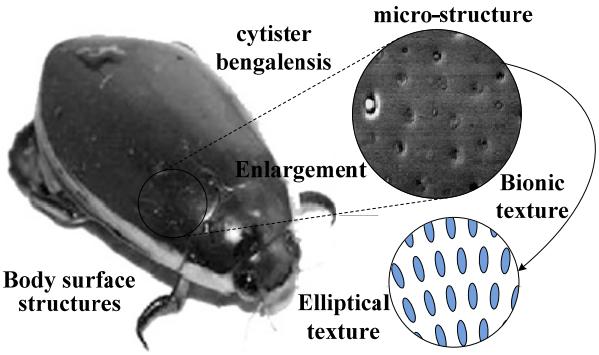

(b) The cytister bengalensis and its micro-structure surface

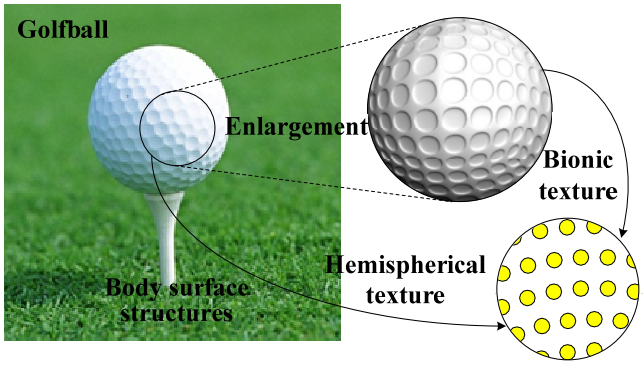

(c) Golfball with bionic concave surface texture

Fig.1. Surface morphology with the function of drag reduction

The actual structures of the upper and lower specimens were shown in Fig. 2. The upper specimen, standing for the simplified rotor of the valve pair, was designed as a ring with anouter diameter of Φ40 mmand inner diameter of Φ20 mm. The lower specimen, representing the simplified valve plate of the valve pair, was designed as a ring with anouter diameter of Φ43mm and inner diameter of Φ6 mm. Three different kinds of bionic non-smooth units respectively with hemispherical pits, triangular pits and ellipsoidal pits were designed on the surfaces of three lower specimens. For the distributions and sizes of the pits, the bionic non-smooth units with hemispherical pits were evenly distributed on the surface of the lower specimen around the center in the diameters of 22, 26, 30, 34 and 38 mm respectively with the number of 40, 48, 55, 62 and 68; while those units with the triangular and ellipsoidal pits were distributed in 4 circles of the diameters of 23,28,33 and 38 mm, respectively with the number of 48, 58, 68, 78. In this way, the spacings between the pits in the radial and circumferential directions were approximately equal. The detailed size and distribution can be seen from Fig. 3.

In order to exclude the influence of the pit area ratio and pit depth on the experimental results, the pit area occupied by non-smooth surface was kept at about

15% of the whole area and the depth was controlled at about 0.5mm. Therefore, the unit of hemispherical pits has a diameter of 1.0 mm. The cross section of the pit unit with the triangular pit is an equilateral triangle with a side length of 1.4mm, while that of pit unit with the ellipsoidal shape is an ellipse with a long axis of 1.8mm and a short axis of 0.6mm. For distinguishing, the lower specimens with the smooth surface, the hemispherical pits surface, the triangular pits surface and the ellipsoidal pits surface were denoted as the type A, B, C and D, respectively (Fig.3).

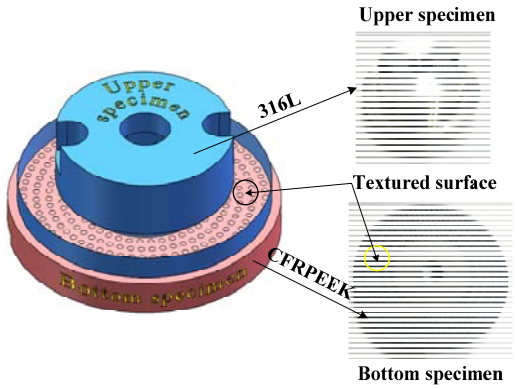

Fig.2. Schematic diagram of textured friction pair

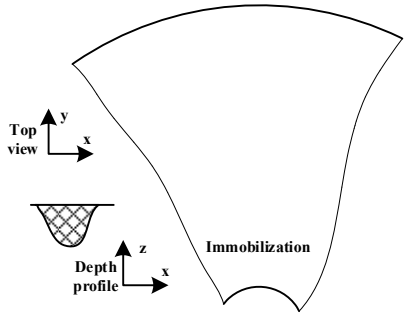

A (Lower specimen with smooth surface)

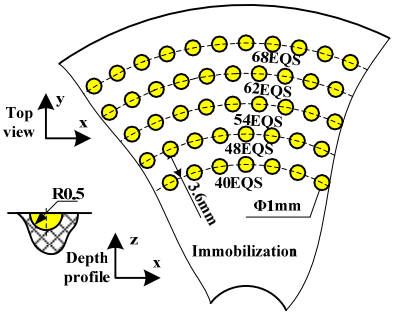

B (Lower specimen with hemispherical pit surface)

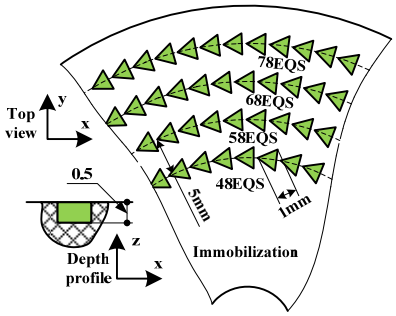

C (Lower specimen with triangular pit surface)

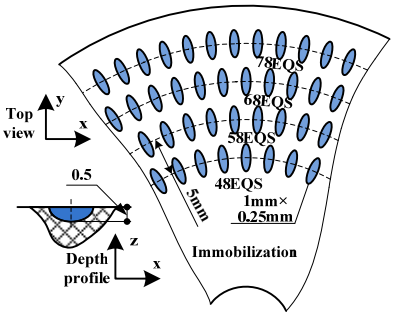

D(Lower specimen with ellipsoidal pit surface)

Fig.3.The distributions and sizes of lower specimens

2.3 Lubricant

Natural seawater, as the lubricant of low-speed and high-torque hydraulic motor, was used in the experiment, and the seawater had pH of 7.2 and salinity of 2.983%，measured according to the GB 17378.4-2007 standard [37]. Before the test, seawater was stood for 24 h, and filter paper was used to remove excessive crystal salt and impurities from it.

2.4 Friction and wear test

In the preparation stage of the test, all the specimens were cleaned with acetone solvent in the ultrasonic cleaner for 30 minutes. Then the specimens were dried off and cleaned with the high-pressure dust removal gas tank to ensure that there were no residual impurities on the surface and pits of the specimens. Subsequently, each of the specimens was weighed and recorded by an electronic balance with an accuracy of 0.1mg for five times, and then the average value was calculated. Finally, to obtain the parameters of the surface morphology and roughness of friction pairs, optical three-dimensional surface measuring instrument (Infinite Focus from Company Alicona) was used to scan the surfaces; and the three-dimensional morphology of smooth surface and bionic non-smooth surfaces with different pit shapes were shown in Fig. 4. Before each test, the upper and lower specimens were immersed in the organic glass cup filled with 100±5mL seawater.

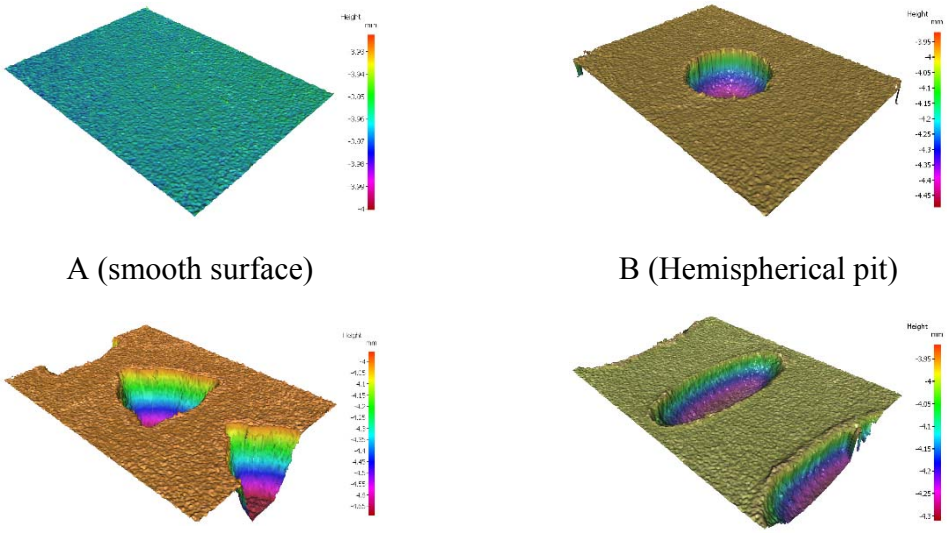

A (smooth surface) B (Hemispherical pit)

C (Triangular pit) D (Ellipsoidal pit)

Fig.4. Three-dimensional morphology of smooth surface and bionic non-smooth surfaces with different pit shapes

The MMD-5A multi-function friction and wear tester was used to test all the specimens, whose principle was shown Fig.5. Before the test, the upper specimen was installed on the spindle and the fixture of the upper specimen had the function of automatic adjustment to ensure that the friction pair kept in contact. Then the lower specimen was installed on the base. The amount of seawater injected into the water box exceeded the upper surface of the fixture to ensure that the surface of the friction pair was always in the state of seawater lubrication during the test. In the meanwhile, the upper specimen was driven by a servo motor to simulate the rotation, and the lower specimen was controlled by the hydraulic cylinder under the testbed to rise and fall for applying load. The sensor and the computer monitored and recorded the friction coefficient in real time. During the test, the load was set to 100N, while the rotational speed was 100r/min and the test lasted for 1 hour.

After the test, the specimens were cleaned, dried off, weighed and the surface was observed againin the same procedure as the preparation stage of the experiment. Before being cleaned again, the pits should be cleaned with small brush and sprayed by high-pressure air to keep away from abrasive debris. What's more, all specimens were dried off for 24 h to eliminate the influence of water absorption on the weighing results.

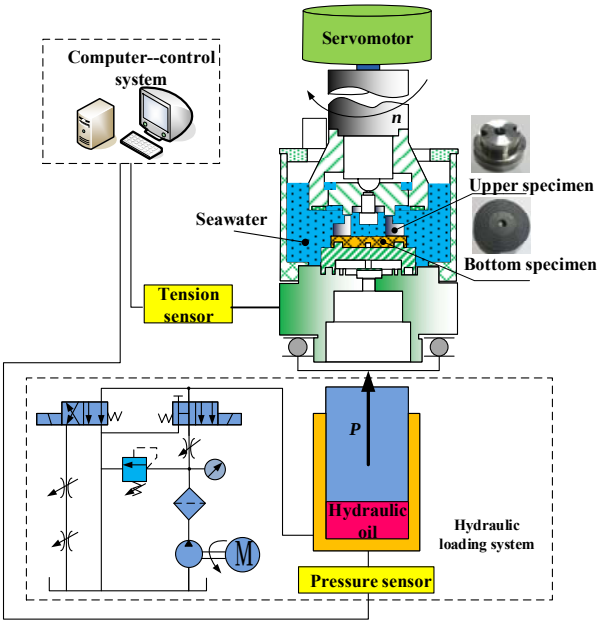

Fig.5. Schematic diagram of MMD-5A friction and wear tester and installation drawing of ring-on-disc tester

3. Results and discussion

3.1 Analysis of friction coefficient

The curves of friction coefficients of friction pairs with smooth surface and three non-smooth surfaces under seawater lubrication varying with time were shown in Fig. 6. It can be seen from the figure that at the beginning of the experiment, the friction coefficient of smooth surface gradually decreased from about 0.11 to about 0.06, and then repeated a similar tendency of a sudden jump followed by a period of stabilization around 0.06 for several times.

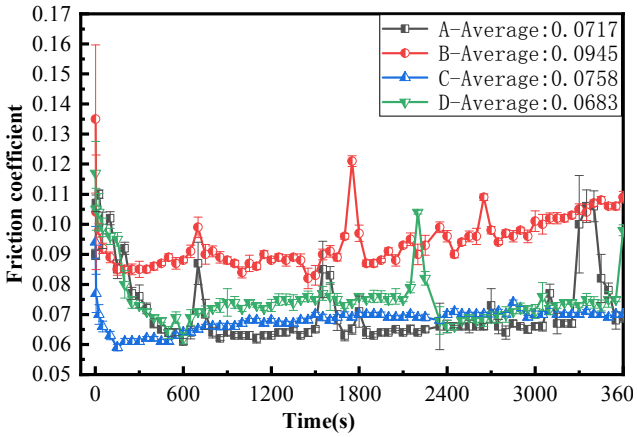

Fig.6. Variation of friction coefficient with test time on smooth and different non-smooth surfaces

However, the friction coefficients of non-smooth surfaces with different morphologies showed different trends from that of the smooth surface. To be specific, the overall friction coefficient of the surface with hemispherical pit was higher than that of the smooth surface along with a tendency of gradual increase at the late stage of the experiment. In addition, the friction coefficient of the surface with triangular pitgenerally was close and showed an analogous trend to that of smooth surface, and that of the surface with ellipsoidal pit surface kept steady with no obvious fluctuation. On the other hand, during the initial period of the experiment, the friction coefficients of all specimens decreased dramatically. The reason is that the frictional behavior was unstable at the beginning of the experiment due to the micro-convex bodies between the contact surfaces of the friction pairs; with the relative movement of the surfaces of the friction pair, the micro-convex bodies fell off with a result of decreased roughness

and friction coefficient.

On the whole, the stability of friction coefficients of non-smooth surface was better than that of the smooth surface owing to the more jumps exhibited in the friction coefficient curve of the smooth surface, which was confirmed by the calculated variance of the friction coefficients for different surfaces (the variances for smooth surface, surface with hemispherical pit, surface with triangular pit and surface with ellipsoidal pit were 1.6×10^{-4}, 8.3×10^{-5}, 9.9×10^{-5} and 1.9×10^{-5} respectively). On the other hand, the fluctuation in the friction coefficients was mainly related to the lubrication condition of the friction pair. When the relative motion of the friction pair became unstable, the water film that was initially existing between the friction pair may get destroyed, which would change the originally full lubrication state into boundary lubrication or even dry friction, resulting in the increase of friction coefficient. This indicated that surface pits could have the potential of storing up the seawater and thus offering sustainable lubrication.

3.2 Analysis of wear property

After the test, the depth of the wear track on the lower specimen was measured using a digital thickness gauge. The corresponding wear volume loss ΔV (mm^3) of the specimen was obtained by measuring the depth of the wear scar. Finally, the wear-resistant property of CFRPEEK with smooth and non-smooth surfaces could be judged by the specific wear rate ω ($mm^3/(N\cdot m)$, which was calculated as follows

$$\omega = \frac{\Delta V}{2\pi ntRF} = \frac{\left(d_1^{\,2} - d_2^{\,2}\right)h}{8ntRF} \tag{1}$$

where n is rotational velocity (r/min), t is wear time (min), R is the mean radius of the upper specimens ring (mm), F is the load (N), d_1 is the diameter of outer grinding circle (mm), d_2 is the diameter of inner grinding circle (mm) and h is the wear depth (mm).

The specific wear rates of the lower specimens with smooth and non-smooth surface were calculated using Eq. (1), as illustrated in Fig.7, to investigate the wear extent of the specimens.

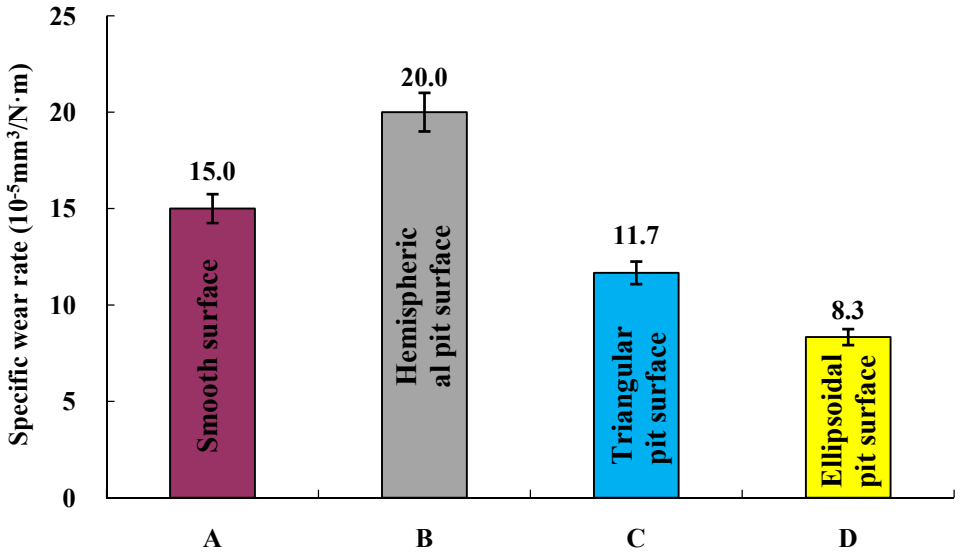

Fig.7. The specific wear rates of lower specimens

The results presented in Fig.7 show that the reasonable non-smooth surfaces could lead to a great improvement in the wear resistance of lower specimens. Amongst all specimens, samples D (the surface with ellipsoidal pit) exhibits the lowest wear rate of 8.3×10^{-5} mm^3·(N·m)$^{-1}$, while sample B (the surface with hemispherical pit) shows the highest of 20×10^{-5} mm^3·(N·m)$^{-1}$,which is about 2.4 times the minimum value. The sequence of specific wear rate for 4 different surfaces is: sample D (the surface with ellipsoidal pit)< sample C (the surface with triangular pit)< sample A (smooth surface) < sample B (the surface with hemispherical pit). This indicates that the shape of non-smooth surfaces plays an important role in reducing the wear rate of PTFE.

The results of mass change for the upper and lower specimens before and after the test were also summarized, which indicated the wear amount of both specimens, as shown in Fig.8. Generally speaking, the masses of all the lower specimens were reduced after grinding, and the wear amount of the non-smooth surface specimens with hemispherical pits was significantly greater than that of the others, while the wear amount of non-smooth surface with the ellipsoidal pits and triangular pits was slightly lower than that of the smooth surface.

It is noteworthy that the mass of specimens with smooth surfaces was increased

and all the specimens were dried off for 24 hours after the test to eliminate the effect of water absorption of the material on the mass. This indicated the possibility of adhesive wear during the grinding of friction pair with smooth surfaces. On the contrary, the masses of specimens with non-smooth surfaces were decreased rather than increased. This may be explained by the fact that the surface textures increased the thickness of the water film, which reduced the adhesion force at the interface, thereby changing the contact state of the interface and reducing the adhesion wear.

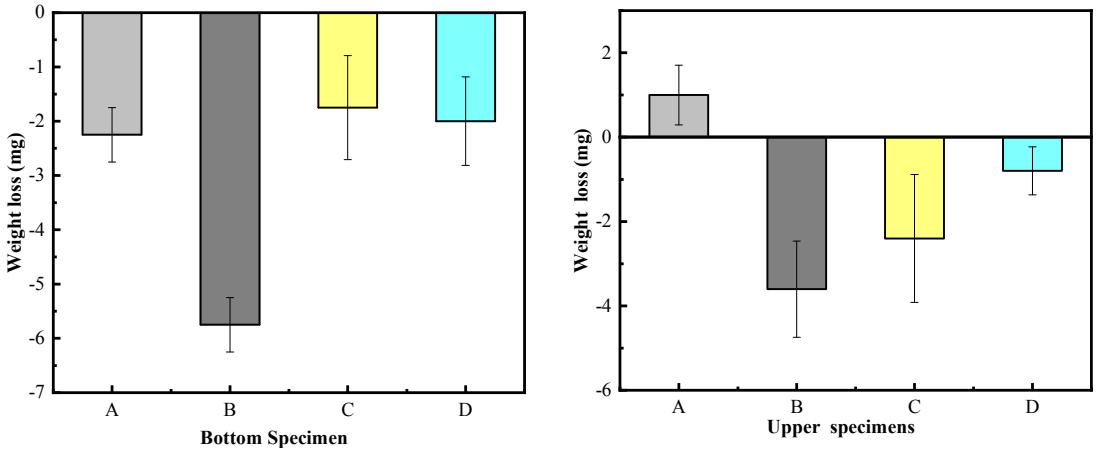

(a) Lower specimens (b) Upper specimens

Fig.8. The results of mass change for the upper and lower specimens

3.3 Analysis of friction and wear process

In this section, the friction and wear process was to be discussed. The material of the upper specimen was 316L, which had a high hardness and a small amount of wear, so the analysis was mainly focused on the wear condition of the lower specimen with the material of CFRPEEK. To analyze in combination with Fig. 6, it can be seen that the rough peaks of the surfaces with 316L and CFRPEEK would contact with or embed in each other under the load at the beginning of the test. When the upper and lower specimens slided relative to each other, the rough peaks would collide with each other violently, thereby increasing the friction coefficient. Since the hardness of 316L is greater than CFRPEEK, the rough peak of CFRPEEK was gradually scraped away and flattened. The most likely cause for running-in can be that the temporal decrease in roughness led to the formation of a polymer transfer film or hydrodynamics.

On the one hand, when roughness decreased as the increase of the running time,

the actual contact area increased and the contact pressure decreased. Starting from boundary lubrication, friction should be decreased until hydrodynamics began. At the same time as the reduction of friction, the wear rate should be decreased due to the separation of the two solids by the formed seawater film.

On the other hand, rough peaks of the surface of 316L began to be embedded in the surface of CFRPEEK, push its material to make it flow plastically and plow out grooves in the subsequent sliding, which was the so-called ploughing effect. With the increase of debris entrapped between the friction pairs, abrasive wear began to occur. When the bonding strength between interfaces was greater than that between CFRPEEK molecules, the surface material of CFRPEEK was transferred to the surface of 316L, which indicated the occurrence of adhesive wear. An important feature of adhesion wear is the transfer of material from the soft CFRPEEK polymer to the hard 316L stainless steel. At first, the material of CFRPEEK was transferred to 316L, then the CFRPEEK was adhered to the polymer transfer film that was attached to the surface of 316L, and then the polymer was stripped off to produce the debris of the transfer film. At the same time, the original transfer film fell off after being fragmented into debris, thereby forming a process in which the material was gradually lost. When the CFRPEEK transfer film that was attached to the surface of 316L reached a certain amount, the friction between the friction pairs was to a certain extent equivalent to be taking place between two surfaces both with CFRPEEK, thereby reducing the friction coefficient and wear rate.

On the contrary, the tribological system would be still in a wear state with high friction provided that the establishment of such a material transfer process was not successful. Unlike the smooth surface, the pits on the non-smooth surfaces can be used to store abrasive debris, which can reduce abrasive wear to a certain extent, and may also delay or destroy the formation of transfer film. This may be one of the reasons why the friction coefficient of the textured surface was larger than that of the smooth surface from 600s to 2400 s.

In order to explain the friction mechanism of the test friction pairs, the wear scars and traces on the upper and lower specimens were investigated by an optical surface measuring instrument. In Figs.9, the worn surfaces of upper specimen were presented. As can be seen, when the friction pair was 316L against the smooth surface

of CFRPEEK (sample A), some fine scratches were noted on the worn surface. Sliding against the surface with hemispherical pit (sample B), the worn surface of 316L exhibited serious wear and turned rougher, as shown in Fig. 9(b). Sliding against the surface with triangular pit (sample C), some wider scratches and grooves were detected, as shown in Fig. 9(c). Sliding against the surface with ellipsoidal pit(sample D), the worn surface of 316L has become smoother and finer, as shown in Fig. 9(d). This indicates the surface with ellipsoidal pit could greatly improve the wear performance.

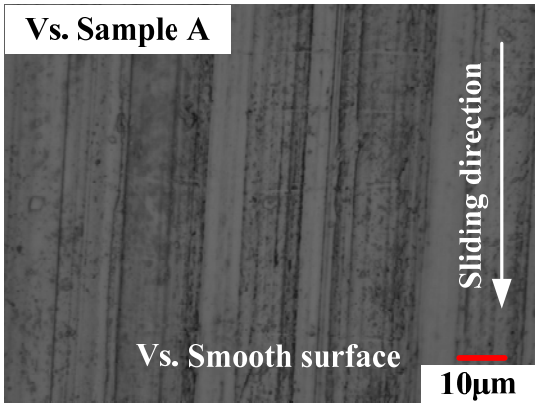

(a) Worn morphology of 316L sliding against sample A

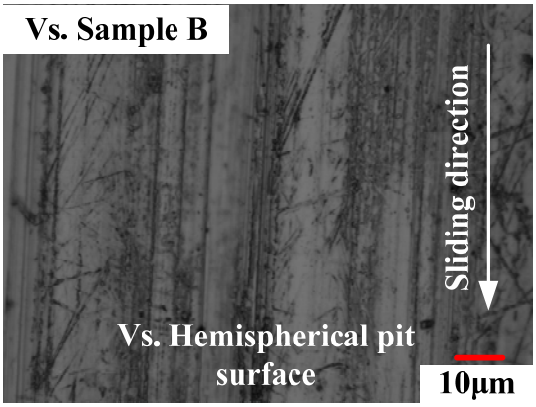

(b) Worn morphology of 316L sliding against sample B

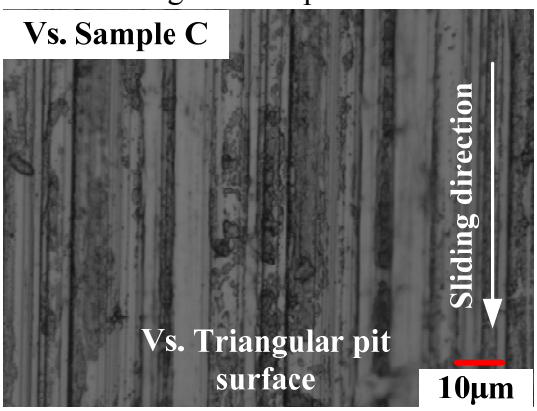

(c) Worn morphology of 316L sliding against sample C

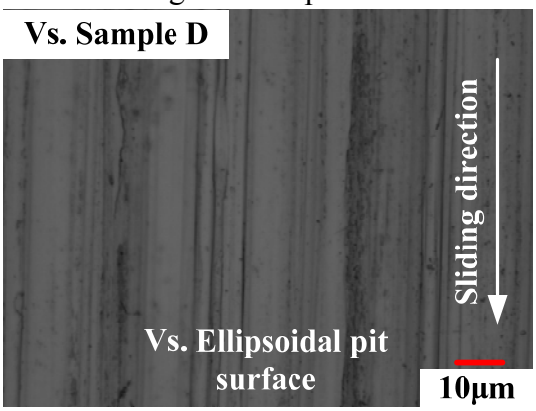

(d) Worn morphology of 316L sliding against sample D

Fig.9. Worn morphologies of upper specimens

Fig. 10(a)~Fig. 10(d) showed the worn morphology of the lower specimens. It can be seen from the worn morphology of the friction pairs that there were obvious grooves along the sliding direction on the surfaces of the lower specimens. Compared with the smooth surface, it can be found that the furrow on the surface with hemispherical pit was wider, and that on the surface with ellipsoidal pit was narrower.

Furthermore, the bright colors at the edges of the pits indicated that they were worn heavily. This is because the edges of the pits were sharp and could behave as 'cutting edges' that scratched the other surface, resulting in the concentration of stress along with wear [38]. In the meanwhile, the micro-cutting effect at the the edges of the pits increased the friction coefficient [39-40].

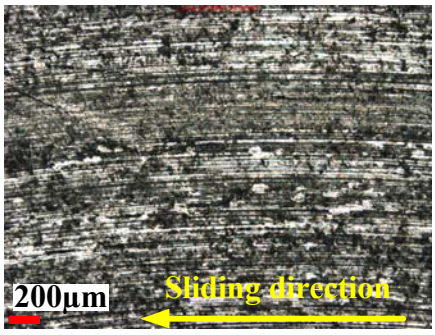

(a) Worn morphology of smooth surface

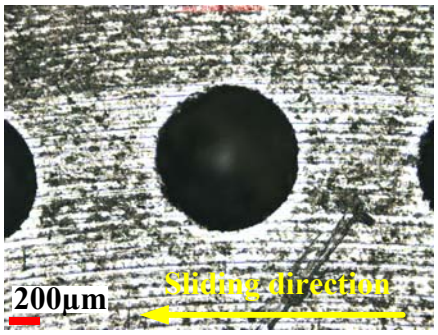

(b) Worn morphology of the surface with hemispherical pit

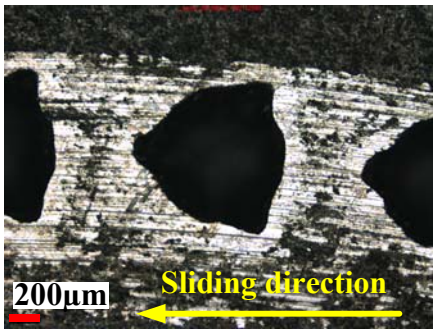

(c) Worn morphology of the surface with triangular pit

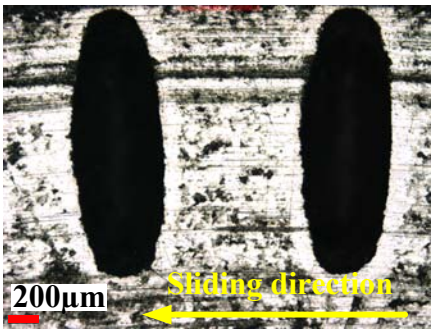

(d) Worn morphology of the surface with ellipsoidal pit

Fig.10. Worn morphologies of the lower specimens

By observing the microscopic morphology of the surfaces, as shown in Fig. 11(a) ~ 9(e), the specific changes on the surfaces were studied. As can be seen from Fig. 11(a), the microscopic morphology of the original surface was not flat (the bright spots in the picture were the reflected light of the bare convex of carbon fibers). In Fig. 11(b), the surface of worn smooth surface became smoother and flatter with uniform wear scars. What's more, the small carbon fibers that were originally unnoticeable appeared as blocky white bright spots due to being worn, and a small amount of yellow debris remained on the rough peak.

Compared with Fig. 11(b), the worn surface with hemispherical pit in Fig. 11(c) was rough with a large amount of debris appearing, which indicated that the surface

with hemispherical pit was worn seriously. Once the dimpled surface was wore out, the lubrication effect was weakened and the friction coefficient rose. Part of the worn surface with triangular pit in Fig. 11(d) exhibited the same 'polishing' phenomenon as the smooth surface, but there were still a large number of substrates that had not been worn out. In Fig. 11(e), there was some debris evenly distributed on the worn surface with ellipsoidal pit, but with no obvious wear observed, which indicated that a relatively uniform transfer film was formed on the surface, as shown in the SEM image of worn surface with ellipsoidal pit (Fig. 11(f)).

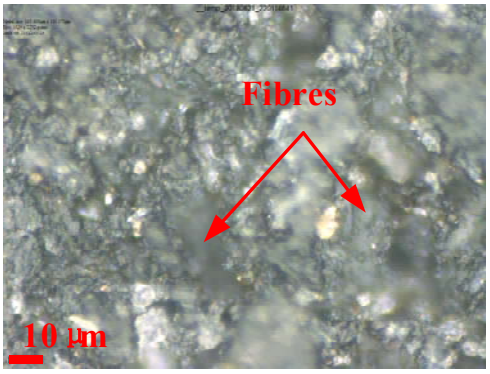

(a) Original surface

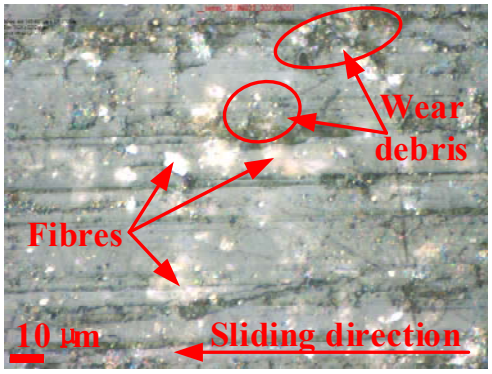

(b) Worn smooth surface

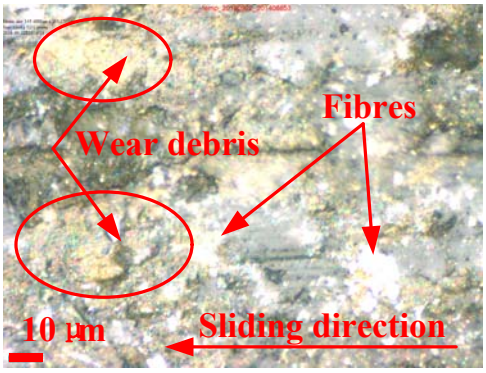

(c) Worn surface with hemispherical pit

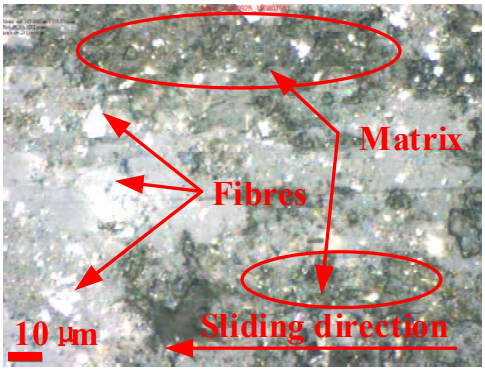

(d) Worn surface with triangular pit

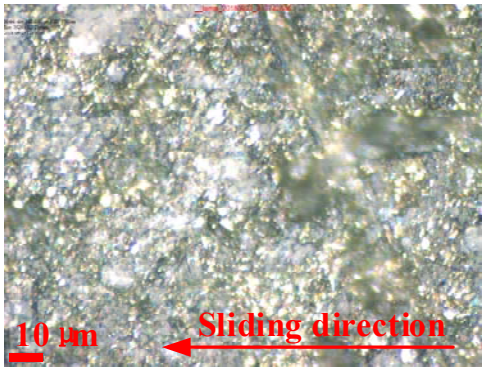

(e) Worn surface with ellipsoidal pit

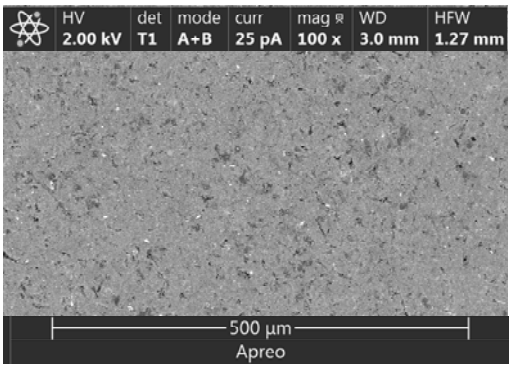

(f) SEM image of worn surface with ellipsoidal pit

Fig.11. The morphologies of the original and worn surfaces of lower specimens

The change of surface roughness is an important index for measuring whether the friction and wear performance of the material is good or not. To further investigate the specific changes in worn surfaces, the surface roughness of lower specimens under seawater lubrication was analyzed. Taking the worn surface with the hemispherical pit as an example，the surface roughness of the lower specimens at different locations (five here) was measured by using optical three-dimensional surface measuring instrument, as shown in Fig. 12.

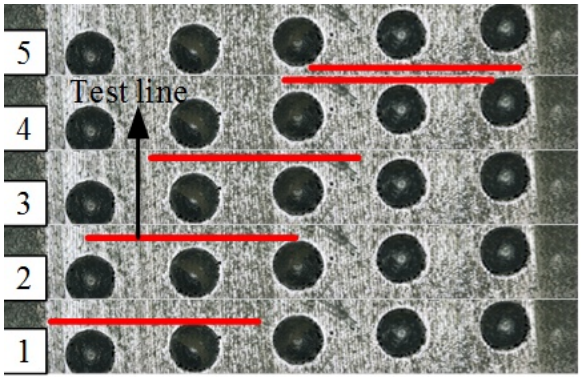

Fig.12. The test lines of roughness at different locations

To study the change of the roughness, the arithmetic mean deviation Ra of the surfaces of the lower specimens was calculated (average of five places) before and after the experiment, as shown in Fig. 13. It can be seen from the figure that the roughness of the smooth surface decreased obviously, while that of the surface with the hemispherical pit increased significantly. The roughness of the other two non-smooth surfaces did not show much change with slight increase for the surface with the triangular pit and slight decrease for the surface with ellipsoidal pit.

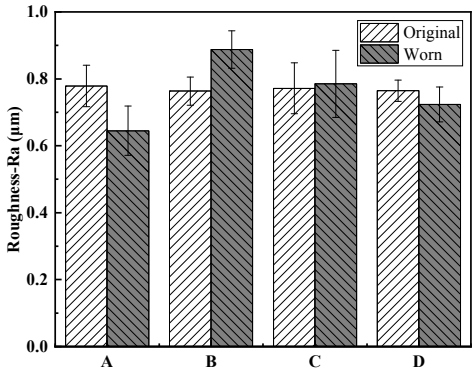

Fig.13. The roughness of the original and worn surfaces of lower specimens

For the untextured specimen, the smooth surface did not have the function of

storing abrasive particles, so the abrasive particles wore the surfaces of the friction pair continuously during the wearing process. Consequently, the grooves produced during the initial running-in process were worn by the abrasive particles, which reduced the roughness of the smooth surface. Although the non-smooth surface could store abrasive particles, thereby reducing abrasive wear, the wear was mainly caused by the phenomenon of groove. On the contrary, deep grooves appearing on the worn surface with pits would increase the roughness slightly. Fig.14 showed a statistical diagram of the percentage of different heights on the smooth surfaceand the surface with triangular pit, which confirmed the above conjecture. As can be seen from the figure, there were deeper concaves and higher protrusions on the surface with triangular pit than the smooth surface. When the roughness of the specimens was high, the abrasion and high friction became predominant [3,41], which is why the friction coefficient and wear rate of the specimen with hemispherical pit were the highest among all the specimens.

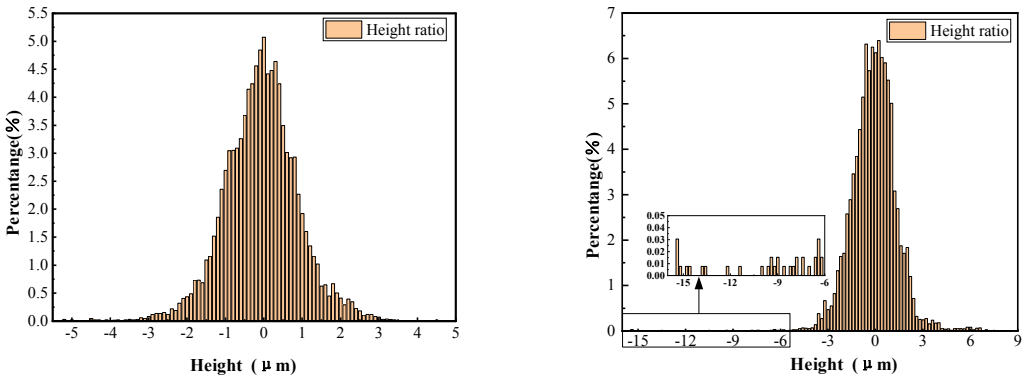

(a) Smooth surface (b) Surface with triangular pit

Fig.14. Histogram of the proportion of different heights

Based on the friction coefficient, wear rate, the surface topography and the roughness of the specimens, it can be found that the surface with ellipsoidal pit had the best tribological performance, followed by the surface with triangular pit, and the surface with hemispherical pit was the worst and even worse than the smooth surface. What is more, it can be found that the friction and wear properties have a high dependence on the shape of the pits. Comparing the lengths of the three kinds of pits perpendicular to the sliding direction, it can be seen that the length of the ellipsoidal pit is the largest, followed by the triangular pit, finally the hemispherical pit, which is coincided with the experimental results. This indicated that the ellipsoidal pit may

improve the pressure distribution of lubricating water film and increase the carrying capacity of water film as well. Segu et al. [42] also found that elliptical pits induced a faster transition of the lubrication state and resulted in a reduced friction coefficient for conformal conditions.

3.4 Wear mechanism of textured surface

According to our previous study [43], the residual pressing force of the port plate pair is marginal. Under low load, it is convenient to form and maintain a stable lubrication film between the stainless steel 316L and CFRPEEK. As illustrated in Fig. 15(a), the clearance between the sliding surfaces at the beginning is filled with adequate seawater. The textured surfaces can trap wear debris and reduce overall contact area so that the surface may be protected from scratch/being stuck by the friction between these particles/debris and the probability of adhesive wear may be diminished. In addition, the hydrodynamic pressure effect of the surface texture will increase the fit clearance, which could promote the sliding friction of the abrasive particles to rolling friction, form the secondary lubrication and reduce the wear and friction.

As the test progresses, the clearance between the sliding surfaces is more and more small, the contact area became the dominant factor of the friction. Although pits can capture the abrasive particles and reduce the action time, the micro-cutting effect at the edge of pits may bring more abrasive particles to the frictional interface, thereby increasing the friction, as shown in Fig.15(b).

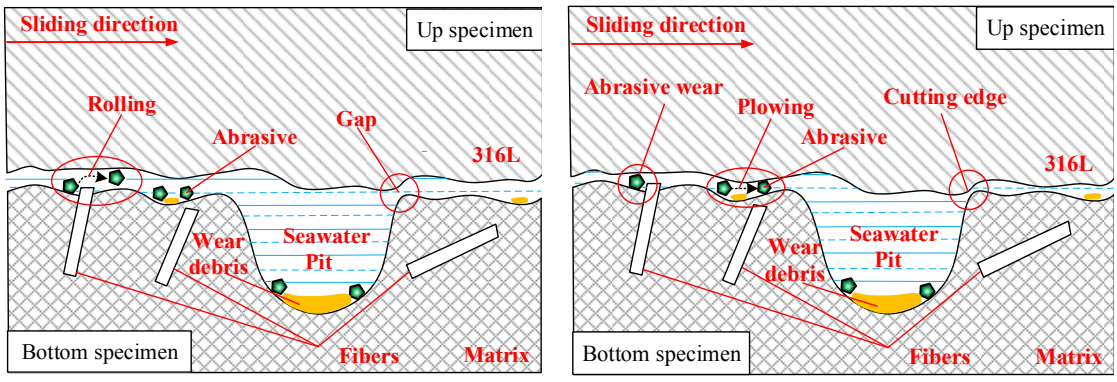

(a) High film (b) Small film

Fig.15. Schematic diagram of wear mechanism of CFRPEEKR with textured surface coupled with 316L

4. Conclusions

A comparative investigation into the tribological behavior of different bionic non-smooth surface textures under natural seawater lubrication was carried out in this study with the friction coefficients evaluated and the worn surfaces of the specimens analyzed. The following conclusions drawn from the tribological experiments can be summarized as:

(1) The stability of friction coefficient of non-smooth surface was better than that of the smooth surface, which was confirmed by the calculated variance of the friction coefficients for different surfaces. And the variances of the friction coefficients for different surfaces were ranked as: surface with ellipsoidal pit (1.9×10^{-5}) <surface with hemispherical pit (8.3×10^{-5}) <surface with triangular pit (9.9×10^{-5}) < smooth surface (1.6×10^{-4}).

(2) The reasonable non-smooth unit can effectively store seawater and debris, and produce hydrodynamic lubrication effect, which reduced adhesion wear as well as prevented direct contact between the frictional surfaces. Therefore, the reasonable design can improve the frictional performance of the surface, and vice versa.

(3) Among the 4 samples, sample D (the surface with ellipsoidal pit) had the lowest friction coefficient and the best anti-wear effect, while there was the phenomenon of high friction and high wear appearing on the surface with hemispherical pit (sample B). Therefore, it could be concluded that the shapes are significant for good tribological performance.

Acknowledgements

The project was financially supported by the National Natural Science Foundation of China (Grant no. 51505111) and the Natural Science Foundation of Zhejiang Province (LQ16E050003).

References

[1] Strmčnik E, Majdič F, Kalin M. Water-lubricated behaviour of AISI 440C stainless steel and a DLC coating for an orbital hydraulic motor application. Tribol Int 2019; 131: 128-36.

[2] Lu XD, Zhao J, Mo JL, Zhang Q, Zhang X, Zhou ZR. Improvement of dynamical and tribological properties of friction systems by introducing parallel-grooved

structures in elastic damping components. Compos Strct 2018; 192: 8-19.

[3] Wang ZQ, Gao DR. Friction and wear properties of stainless steel sliding against polyetheretherketone and carbon-fiber-reinforced polyetheretherketone under natural seawater lubrication. Mater Design 2014; 53: 881-7.

[4] Friedrich K, Davim JP. Wear of advanced materials. London: ISTE-Wiley; 2012.

[5] Abdel-Aal HA, Mansori ME, Zahouani H. A comparative study of frictional response of shed snakeskin and human skin. Wear 2017; 376-377: 281-94.

[6] Dean B, Bhushan B. Shark-skin surfaces for fluid-drag reduction in turbulent flow: A review. Philos T R Soc A 2010; 368: 4775-806.

[7] Yu M, Hermann I, Dai Z, Gitis N. Mechanical and frictional properties of the elytra of five species of beetles. J Bionic Eng 2013; 10: 77-83.

[8] Lu X, Khonsari MM. An experimental investigation of dimple effect on the stribeck curve of journal bearings. Tribol Lett 2007; 27: 169-76.

[9] Usman A, Park CW. Optimizing the tribological performance of textured Piston ring- liner contact for reduced frictional losses in SI engine: Warm operating conditions. Tribol Int 2016; 99: 224-36.

[10] Ayadi K, Brunetière N, Tournerie B, Maoui A. Experimental and numerical study of the lubrication regimes of a liquid mechanical seal. Tribol Int 2015; 92: 96-108.

[11] Sugihara T, Enomoto T. Performance of cutting tools with dimple textured surfaces: A comparative study of different texture patterns. Precis Eng 2017; 49: 52–60.

[12] Wakuda M, Y Yamauchi, Kanzaki S, Yasuda Y. Effect of surface texturing on friction reduction between ceramic and steel materials under lubricated sliding contact, Wear 2003; 254: 356-63.

[13] Gachot C, Rosenkranz A, Hsu SM, Costa HL. A critical assessment of surface texturing for friction and wear improvement. Wear 2017; 372-373: 21-41.

[14] Zhang H, Hua M, Dong GZ, Zhang DY, Chen WJ, Dong GN. Optimization of texture shape based on genetic algorithm under unidirectional sliding. Tribol Int 2017; 115: 222-32.

[15] Ibatan T, Uddin MS, Chowdhury MAK. Recent development on surface texturing in enhancing tribological performance of bearing sliders. Surf Coat Tech 2015; 272: 102-20.

[16] Sun QC, Hu TC, Fan HZ, Zhang YS, Hu LT. Dry sliding wear behavior of TC11

alloy at 500°C: Influence of laser surface texturing. Tribol Int 2015; 92: 136-45.

[17] Wos S, Koszela W, Pawlus P. The effect of both surfaces textured on improvement of tribological properties of sliding elements. Tribol Int 2016; 113: 182-8.

[18] Lu P, Wood RJK, Gee MG, Wang L, Pflfleging W. The use of anisotropic texturing for control of directional friction. Tribol Int 2017; 113: 169-81.

[19] Qiu M, Minson BR, Raeymaekers B. The effect of texture shape on the friction coefficient and stiffness of gas-lubricated parallel slider bearings. Tribol Int 2013; 67: 278–88

[20] Chen P, Xiang X, Shao T, La YQ, Li JL. Effect of triangular texture on the tribological performance of die steel with TiN coatings under lubricated sliding condition. Appl Surf Sci 2016; 389: 361-68.

[21] Qiu Y, Khonsari MM. Experimental investigation of tribological performance of laser textured stainless steel rings. Tribol Int 2011; 44: 635-44.

[22] Shen C, Khonsari MM. Effect of dimple's internal structure on hydrodynamic lubrication. Tribol Lett 2013; 52: 415-30.

[23] Fowell MT, Medina S, Olver AV, Spikes HA, Pegg IG. Parametric study of texturing in convergent bearings. Tribol Int 2012; 52: 7-16.

[24] Xing Y, Deng J, Wu Z, Wu FF. High friction and low wear properties of laser-textured ceramic surface under dry friction. Opt Laser Technol 2017; 93: 24-32.

[25] Yu HW, Huang W, Wang XL. Dimple patterns design for different circumstances. Lubr Sci 2013; 25: 67-78.

[26] Yin B, Li X, Y Fu, Fu YH, Yun W. Effect of laser textured dimples on the lubrication performance of cylinder liner in diesel engine. Lubrication Science 2012; 24: 293-312.

[27] Pettersson U, Jacobson S. Friction and wear properties of micro textured DLC coated surfaces in boundary lubricated sliding. Tribol Lett 2004; 17: 553-9.

[28] Cui FZ, Luo ZS. Biomaterials modification by ion-beam processing. Surf Coat Tech 1999; 112: 278-85.

[29] Wang XL, Adachi K, Otsuka K, Kato K. Optimization of the surface texture for silicon carbide sliding in water. Appl Surf Sci 2006; 253: 1282-6.

[30] Ryk G, Etsion I. Testing piston rings with partial laser surface texturing for friction reduction.Wear 2006; 261: 792-6.

[31] Li K, Yao Z, Hu Y, Gu WB. Friction and wear performance of laser peen textured surface under starved lubrication. Tribol Int 2014; 77: 97-105.

[32] Yamakiri H, Sasaki S, Kurita T, N Kasashima. Effects of laser surface texturing on friction behavior of silicon nitride under lubrication with water. Tribol Int 2011; 44: 579-84.

[33] Davim JP. Progress in green tribology. Berlin: DE Gruyter; 2017

[34] Davim JP, Rosária C. Effect of the reinforcement (carbon or glass fibres) on friction and wear behaviour of the PEEK against steel surface at long dry sliding. Wear 2009; 266: 795-9.

[35] Zhou CH, Ren LQ, Zhang R, Wang SJ, Zhao WF. The relationship between body surface structure of cytisterbengalensis and its function of deducing risistance. J Northeast Normal U 2006; 38: 109-13.

[36] Aoki K, Muto K, Okanaga H. Aerodynamic characteristics and flow pattern of a golf ball with rotation. Procedia Eng 2010; 2: 2431-6.

[37] GB 17378.4-2007. The specifications for marine monitoring-Part 4: Seawater analysis. Beijing: Standards Press of China; 2008.

[38] Wang XS, Giovannini M, Xing YQ, Kang M, Ehmann K. Fabrication and tribological behaviors of corner-cube-like dimple arrays produced by laser surface texturing on medical needles. Tribol Int 2015; 92: 553-8.

[39] Korpela T, Suvanto M, Pakkanen TT. Friction and wear of periodically micro-patterned polypropylene in dry sliding. Wear 2012; 289: 1-8.

[40] Gachot C, Rosenkranz A, Hsu SM, Costa HL. A critical assessment of surface texturing for friction and wear improvement. Wear 2017; 372-373: 21-41.

[41] Davim JP, Marques N, Baptista AM. Effect of carbon fibre reinforcement in the frictional behaviour of Peek in a water lubricated environment. Wear 2001; 250: 1100-4.

[42] Segu DZ, Choi SG, Choi JH, Choi JH, Kim SS. The effect of multi-scale laser textured surface on lubrication regime. Appl Surf Sci 2013; 270: 58-63.

[43] Wang ZQ, Gao DR. Thrust collar parameter optimization of water hydraulic motor based on orthogonal test. Chin Mech Eng 2013; 24: 3360-3365.